AIR POLLUTION AND OTHER ENVIRONMENTAL STRESSES: GASEOUS NO_2 EXPOSURE LEADS TO SPECIFIC ALTERATIONS OF *PSEUDOMONAS FLUORESCENS*

THIBAULT CHAUTRAND[1], DJOUHAR SOUAK[1], TATIANA KONDAKOVA[2], SÉGOLÈNE DEPAYRAS[1], NADINE MERLET-MACHOUR[3], HERMANN J. HEIPIEPER[4], MARC G. J. FEUILLOLEY[1], NICOLE ORANGE[1] & CÉCILE DUCLAIROIR-POC[1]
[1]Laboratory of Microbiology Signals and Microenvironment, EA4312, Normandy Univ., Univ. Rouen, France
[2]LPS-BIOSCIENCES SAS, Domaine de l'Université Paris Sud, France
[3]UMR 6014 COBRA, Normandy Univ., Univ. Rouen, France
[4]Department of Environmental Biotechnology, UFZ Helmholtz Centre for Environmental Research, Germany

ABSTRACT

In the environment, microorganisms are subjected to a wide range of stresses. These stresses can be of natural origin, like temperature variations and ultraviolet exposure, but can also originate from humans like air pollution. The effects of air pollution on humans are more and more studied and reveal increasing concerns for human health, including augmentations of respiratory infections. However, the microbial responses to atmospheric pollution are still largely unknown. In a similar fashion, few studies investigate the effects of UV radiation on microorganisms. As NO_2 is an air pollutant causing nitrosative stress in biological organisms by reacting with various biological molecules, solar UV radiations are also an important environmental source of cell damage. UVB can directly damage DNA and cause erythema, but only represent 6% of the total UV reaching the earth surface. The 94% others are UVA, that cause oxidative stress in the cells. Since oxidative and nitrosative stresses are interlinked, the exposition of airborne bacteria to these two stresses could have synergistic consequences. In this study, the airborne *Pseudomonas fluorescens* strain MFAF76a was exposed successively to gaseous NO_2 and UV light to assess whether these two environmental stresses have synergistic effects on bacterial physiology. Bacterial growth was assessed by optical density and membrane permeability by flow cytometry. Exposures to successively gaseous NO_2 and UVB light lead to a non-synergistic decrease of bacterial viability. Furthermore, only NO_2 seems to damage the membrane and induces membrane permeabilization. Lipidomic analysis reveals similarities between the lipidic profile of bacteria in their exponential growth phase or for the exposed ones to NO_2 during their stationary growth phase. Furthermore, lipidic alterations show that mechanisms induced by NO_2 differ from those implemented by temperature. In conclusion, this study reveals that bacterial alterations caused by NO_2 are specific, with a strong emphasis on membrane damage.

Keywords: NO_2, ultraviolet, Pseudomonas fluorescens, air pollution, health, bacterial membranes.

1 INTRODUCTION

Air pollution is a world-wide problem for both human health and environment. A major part of current air pollution is the result of human activities such as transport, industry and power plants [1]. Nitrogen dioxide (NO_2) is an air pollutant released by fuel combustion processes. High concentrations of NO_2 are associated with both environmental problems such as photochemical smog and acid rains, as well as health issues such as asthma and bronchitis [1], [2]. NO_2 is a reactive nitrogen species (RNS), along other related molecules such as nitric oxide (NO) and peroxynitrite ($ONOO^-$). RNS can damage various biomolecules such as DNA [3], lipids [4] and proteins [5] by reacting with them and are toxic for biological organisms at high concentrations.

In nature, microorganisms are regularly exposed to a wide range of stresses, such as temperature changes, ultraviolet (UV) exposure, and low water availability. Solar UV

WIT Transactions on Ecology and the Environment, Vol 244, © 2020 WIT Press
www.witpress.com, ISSN 1743-3541 (on-line)
doi:10.2495/AIR200051

radiations are an important cause of cell damage for biological organisms [6]. Ultraviolet B (UVB) have a wavelength comprised between 280 and 315 nm. Exposure to UVB can directly damage DNA, and cause various skin pathologies in human, such as erythema, dermatitis and skin cancer [6]. However, UVB only represent 6% of the total UV reaching the surface, the other 94% being mostly ultraviolet A (UVA), which possess a wavelength comprised between 315 and 400nm. UVA photons carry less energy than UVB photons and do not directly affect the DNA they encounter. Nonetheless, they can cause more oxidative stress in cells. Atmospheric pollution can add to this stress, notably by the nitrosative stress induced by anthropogenic RNS. The effects of air pollution on bacteria is not well studied, and its combination to other environmental stresses even less. Indeed, the addition of multiple environmental stresses could have synergistic effects on bacterial physiology. Since oxidative stress and nitrosative stress are strongly interlinked, the combination of these two stresses could lead to synergistic effects not suspected when they are studied separately. Comprehension of the interactions between air pollution and other environmental stresses on bacteria could help to understand the anthropogenic alterations on environmental microbial communities and their effect on human health.

The *Pseudomonas fluorescens* MFAF76a strain is an airborne environmental bacterium presenting several virulence factors making it a potential human pathogen [7]. These characteristics make it a relevant organism to study in the context of bacterial adaptation to environmental pollution. This study aims to elucidate the relationship between air pollution and other environmental stresses regarding their effect on the physiology of the strain MFAF76a. First, bacteria were successively exposed to gaseous NO_2 and UV light to assess their viability and membrane permeability. The effects of NO_2 on bacterial permeability prompted us to assess the potential impacts of NO_2 on the lipid composition of the strain MFAF76a. To appreciate the specificity of the cell response to NO_2 as an environmental stress, these results were compared to the effects of temperature and growth phase on bacterial lipidic composition. As MFAF76a presents several virulence factors [7] and could potentially adapt to a human host, the temperature studied were the optimal growth temperature of the strain of 28°C and the human body temperature of 37°C.

2 MATERIALS AND METHODS

2.1 Bacterial strain and growth conditions

The bacteria used in this study is the strain *Pseudomonas fluorescens* MFAF76a. This strain was isolated in the Rouen harbor (Normandy, France) from dust clouds generated during crop ship loading [7]. Strain MFAF76a was precultured 24 h at 28°C or 37°C in Lysogeny Broth (LB) (yeast extract 5 g/L, peptone 10 g/L, NaCl 5 g/L). The preculture was used to prepare the culture at a final optical density at 580 nm (OD_{580}) of 0.08 in Davis Minimal Broth (DMB) [8]. Cultures were incubated at 28°C or 37°C under agitation at 180 rpm.

2.2 Exposition to NO_2

After 16 h of incubation at 28°C, bacterial cultures were centrifuged at 13,000 g for 10 min at 4°C and were resuspended in DMB at a final optical density at an OD_{580} of 4. 125 µL of bacteria were deposited on cellulose acetate filters (pore size 0.2 µm, Sartorius Stedim Biotech GmbH, Göttingen, Germany). The filters were then deposited on Petri dishes containing DMB with 15 g/L agar. Bacteria were incubated 4 h at 28°C after which the filters were transferred on 15 g/L agar plates. The agar plates were placed into the gaseous

exposition system developed in the laboratory [9]. Bacteria were exposed to 45 ppm of gaseous NO_2 with a N_2/O_2 ratio of 8/2 or synthetic air for 2 h with a constant gas stream of 2 L/min.

2.3 UV exposure

After exposure to gaseous NO_2, all the agar plates were put to obscurity. One agar plate exposed to NO_2 and one agar plate exposed to synthetic air were placed at the center of the UV exposition chamber (Irradiation chamber BS-03, Opsytech Dr. Gröbel GmbH, Ettlingen, Germany). Bacteria were exposed to either 33 mJ/cm^2 of UVA, 15 mJ/cm^2 of UVB or both. Control bacteria were not exposed to any radiation. Bacteria were then resuspended in sterile physiological water (NaCl 9 g/L).

2.4 Membrane permeability assays

The bacterial suspension after exposure was stained for 15 min with propidium iodine 30 nM (PI) and SYTO9 5.01 nM from the kit Live/Dead Backlight (L-7012, Thermo Fisher Scientific, Saint-Herblain, France). Bacteria were observed using flow cytometry (CytoFLEX S, Beckman Coulter, Villepinte, France) and the Cytexpert v1.2 software (Beckman Coulter, Villepinte, France). PI and SYTO9 were excited at a wavelength of 488nm and their fluorescence emission were detected at 690 ± 50 nm and 525 ± 40 nm respectively. 10,000 events were collected for each measurement at medium flow (30 µl/min). Positive control for membrane permeabilization was performed on bacteria by treating them with 50% ethanol for 10 minutes before staining. The software was calibrated using the positive permeabilization control. Significativity of differences between mean values were assessed using t-test.

2.5 HPTLC-MALDI TOF MSI analysis of glycerophospholipids

The bacterial GP analysis was performed as previously described [10] After exposure and resuspension at $OD_{580} = 2$ in sterile saline solution, bacteria were centrifuged at 4°C (13,000 g) and rinsed three times with sterile saline solution. Aliquots were resuspended in deionized water and lyophilized using a Freeze Dryer Heto PowerDry PL9000-50/ HSC500 (Thermo Fisher Scientific, Saint-Herblain, France). Lipid extraction was performed according to the method of Bligh and Dyer [11]. Bacterial lipid extracts (100 µL) were separated in triplicates on High Performance Thin-Layer Chromatography (HPTLC) plates using $CHCl_3/CH_3CH_2OH/H_2O/N(CH_2CH_3)_3$ (35/35/7/35, v/v/v/v) as mobile phase. The GP spots were visualized by UV fluorescence (365 nm) after labeling with 0.05% primulin dye in acetone/water, (8/2, v/v). Retention factors (R_f) are calculated using the Sweday JustTLC software (v. 4.0.3, Lund, Sweden). Moreover, the following staining was performed in order to identify the lipid classes present in the HPTLC bands: (i) 2% azure A in 1 mM sulfuric acid for sulfatides and sulfoglycolipids, and (ii) 0.25% ninhydrin prepared in acetone-lutidine (9:1, v/v) for phosphatides and lipids having a free amino group. GPs were identified directly on HPTLC plates by Matrix-Assisted Laser Desorption Ionization mass spectrometry – Time of Flight (MALDI-TOF) using an Autoflex III mass spectrometer equipped with a laser Optibeam TM Nd/YAG (355 nm) with a 200-Hz tripled-frequency (Bruker Daltonics, Bremen, Germany). The DHB (200 g/L in acetonitrile/0.1% TFA, 90/10, v/v) was chosen as MALDI matrix. Autoflex III mass spectrometer was run in the reflector positive ion mode using the TLC-MALDI software (v. 1.1.7.0, Bruker Daltonics, Bremen, Germany). The Post Source Decay (PSD) spectra were acquired using FlexControl software (Bruker Daltonics).

The Mass Spectrometry Imaging (MSI) was performed using the FlexImaging software (v. 2.1., Bruker Daltonics, Bremen, Germany). The GP distribution was reconstructed according to the m/z of GPs, identified by MS and PSD spectra in combination with LIPID MAPS database and previously obtained data [10]. Individual lipid spots were labeled by a specific color code according to their m/z.

2.6 Fatty acids analysis

Fatty acid methyl esters were prepared by incubation for 15 min at 95°C in a boron trifluoride (BF_3)/methanol (140 g BF_3 per liter of methanol) and extracted with hexane as described by Morrison and Smith [12]. Fatty acid methyl esters were separated and analyzed by gas chromatography (GC) coupled to flame ionization detection using an Agilent Technology, 6890 Network GC System, 7683 Series Injector equipped with a split/splitless injector. The apparatus was equipped with a CP-Sil 88 capillary column (Chrompack, Middelburg, the Netherlands; length, 50 m; inner diameter, 0.25 mm; 0.25 mm film). FAs were identified by coinjection as internal standards of reference compounds obtained from Supelco (Bellefonte, Pennsylvania, USA) and were quantified on the basis of their peak areas in total ion chromatograms. All experiments were performed in triplicate. The degree of FA saturation was determined as the ratio between the saturated FAs and the unsaturated FAs [13].

3 RESULTS AND DISCUSSION

In the environment, bacteria are submitted to a wide array of stresses, such as variations of temperatures, UV radiation and nitrosative stress through atmospheric pollution. In particular, the effects of the atmospheric pollutant NO_2 on bacteria is poorly understood, and its interaction with other types of environmental stresses even less. In order to study the effects of atmospheric NO_2 on bacteria and its potential modulation by other environmental conditions, the airborne *Pseudomonas fluorescens* strain MFAF76a was exposed to NO_2 or synthetic air for 2 hours, through an exposition system described previously [9], as well as different temperatures and different UV radiations.

3.1 NO_2 and UV exposure induce bacterial mortality through different processes

NO_2 is a RNS, which can cause important damage to biological molecules in a similar fashion to reactive oxygen species (ROS). UV radiation can harm biological organisms through different modes of actions depending mostly on the wavelength of the radiation. UVA-induced damages result mostly from their capacity to induce the formation of ROS in the cell through photochemical reactions with proteins and other cell components [14]. Meanwhile, UVB are more energetic and can mutate DNA by forming pyrimidine dimers at sequences containing 5-methylcytosine, but they induce less oxidative stress in the cell. Since oxidative and nitrosative stresses are highly intertwined, we hypothesized that UV radiation could potentiate the nitrosative stress induced by NO_2. To assess whether this hypothesis was true, *P. fluorescens* MFAF76a growth was followed after exposure to both NO_2 and different UV wavelengths (Fig. 1). NO_2 concentration of 45 ppm correspond to the concentration of NO_2 capable of causing irreversible consequences to human health [15]. Since UVB and UVA have drastically different ways to affect the cell, it is important to differentiate them to understand the bacterial response to this stress. However, most of the information available on the doses received at the surface does not specify the nature of the UV measured. Natural UVB exposure of humans varies widely depending on individuals and their location. Therefore, UV doses that airborne potential pathogens such as the MFAF76a strain are

susceptible to encounter are difficult to assess. Phototherapy can be used to treat skin conditions such as dermatitis, by using UVB doses going from 20 to 200 mJ/cm^2 [16]. This study therefore used an UVB dose of 15 mJ/cm^2, comparable to the lowest doses used in dermatitis treatment. To maintain an equivalent exposure time for both types of UV. Since the UV exposition chamber does not allow modifications of the intensity of UV radiations, total UV exposure depends only of the exposure time. In order to keep this exposure time consistent between conditions, the dose of 33 mJ/cm^2 was used for UVA.

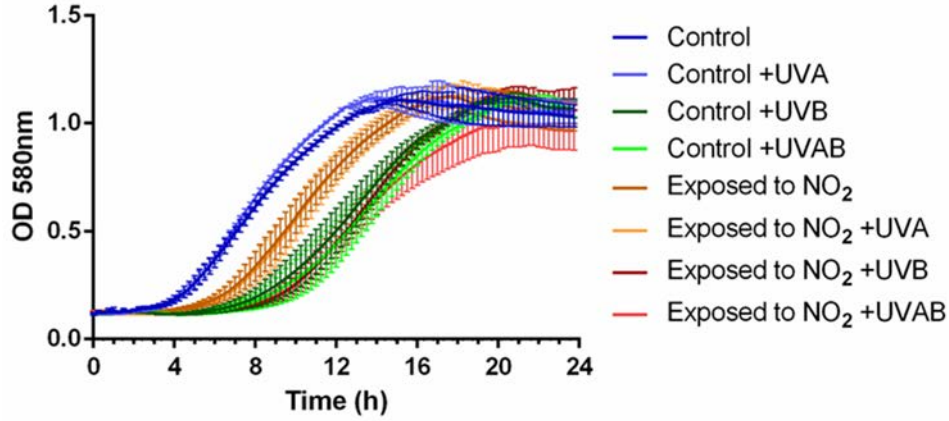

Figure 1: Growth curve of *P. fluorescens* MFAF76a strain after exposure to UV radiations and gaseous NO_2. Bacteria were exposed to either 45 ppm of NO_2 (Exposed to NO_2) or synthetic air (Control). After exposure to NO_2, bacteria were exposed to either 33 mJ/cm^2 of UVA (+UVA), 15 mJ/cm^2 of UVB (+UVB), both 33 mJ/cm^2 of UVA and 15 mJ/cm^2 of UVB (+UVAB) or not exposed to light. Bacterial growth was then monitored through OD_{580} for 24 h. Data represents the means ±SD of three experiments.

While none of the conditions seems to affect the growth rate of the bacteria on the long term, the shift of the growth curves in bacteria exposed to NO_2 and UVB indicates an important mortality rates among bacteria exposed to these conditions. Intriguingly, despite their ability to induce oxidative stress, UVA does not increase mortality even when combined with NO_2. It could be argued that the doses used in this study were not important enough, but similar experiments were done with doses as high as 4 J/cm^2 with no difference (data not shown). Furthermore, even though NO_2 and UVB both induce mortality in MFAF76a strain, the combination of these two stresses does not further increase mortality.

To better understand the mechanisms underlying these independent mortality rates, membrane permeability of bacteria exposed to NO_2 and UV radiation was assessed (Fig. 2).

Permeability assays were realized with the green-fluorescing membrane-permeant DNA probe Syto9 and the red-fluorescing membrane impermeable DNA probe propidium iodide (PI), and their fluorescence was measured by flow cytometry. This labelling reveals three populations, the cells labelled by Syto9 only, not permeabilized, the cells labelled by IP (Syto9- IP+), totally permeabilized, and the cells labelled by both Syto9 and IP (Syto9+ IP+), partially permeabilized. Membrane permeability assays show that only less than 30% of bacteria not exposed to NO_2 are labelled with IP or IP and Syto9, compared to around 70%

of bacteria exposed to NO_2, regardless of UV exposure. Therefore, NO_2 exposure causes an important increase in bacterial membrane permeability, which is usually associated with a reduction of cell viability. UV exposure however does not affect membrane permeability despite the fact that UVB exposure has a stronger negative impact on bacterial viability at the concentrations studied. Lethality induced by UVB is therefore probably linked to DNA alterations and not oxidative stress. This suggests that the mechanisms leading to cell mortality between NO_2 and UVB exposure are unrelated.

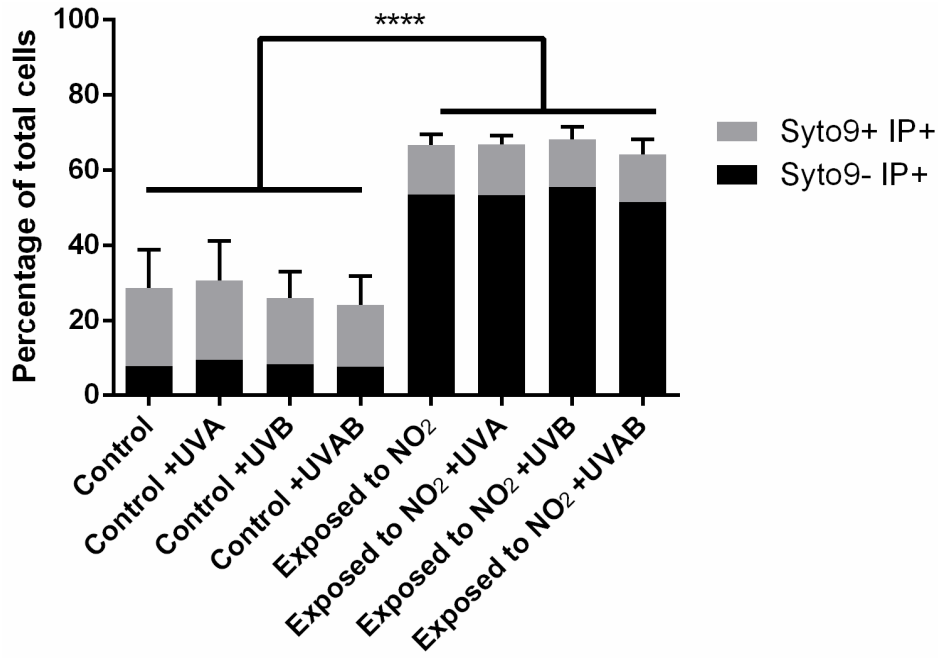

Figure 2: Membrane permeability of MFAF76a after exposure to UV radiations and gaseous NO_2. Bacteria were exposed to either 45 ppm of NO_2 (Exposed to NO_2) or synthetic air (Control). After exposure to NO_2, bacteria were exposed to either 33 mJ/cm^2 of UVA (+UVA), 15 mJ/cm^2 of UVB (+UVB), both 33 mJ/cm^2 of UVA and 15 mJ/cm^2 of UVB (+UVAB) or not exposed to light. Membrane permeability was assessed by cytometry using the Live/Dead Backlight kit (L-7012, Thermofisher) according to the manufacturer recommendations. Data represents the means ±SD of three experiments. Statistical significance of the results was assessed by t-test. ****: p-value <0.0001.

3.2 High NO_2 concentrations lead to a specific alteration of membrane composition.

To assess whether the membrane permeability alterations caused by NO_2 are linked to a reorganization of the bacterial membrane, the lipid composition of MFAF76a was assessed after exposure to NO_2 at different concentrations (Table 1). The impact of NO_2 on bacterial lipidome was assessed at 0.1, 5 and 45 ppm. 0.1 ppm mimics the maximum average exposure to NO_2 recommended by the World Health Organization. 5 ppm mimics the threshold causing

reversible effects on human health, while 45 ppm mimics concentrations causing irreversible effects on human health [2], [15].

Table 1: Effect of NO_2 exposure on glycerophospholipid inventory in *P. fluorescens* MFAF76a strain. The lipid identification was performed on the basis of MS and PSD spectra using LIPID MAPS database and the analysis of lipid standard. The presence of assigned m/z in lipid extract in triplicate is shown by grey squares. The colorless squares show the absence of assigned m/z in lipid extract. The lipid extractions, MS and PSD analysis in all studied conditions were performed in three replicates.

Glycerophospholipid identification						NO_2 level, ppm			
Retention factor	GP class	Species	Molar mass (M), g/mol	m/z	Assignment	0	0.1	5	45
0.24±0.01	PC	PC [16:0 + 16:1]	731.5	732.6	$[PC_1+H]^+$	■	■	■	■
		PC [16:0 + 16:1]	731.5	754.5	$[PC_1+Na]^+$	■	■	■	■
		PC [16:0 + 18:1]	759.6	782.6	$[PC_2+Na]^+$	■			
0.26±0.02	UGP	UGP [16:0 + 17:0]	904.5	927.5	$[UGP_1+Na]^+$	■	■	■	
		UGP [16:0 + 18:0]	918.5	941.5	$[UGP_2+Na]^+$	■	■	■	
		UGP [17:1 + 18:0]	930.5	953.5	$[UGP_3+Na]^+$	■	■	■	
0.43±0.02	PE	PE [16:0 + 16:1]	689.5	712.5	$[PE_1+Na]^+$	■	■	■	■
				734.5	$[PE_1+2Na-H]^+$	■	■	■	■
		PE [16:0 + 17:1]	703.5	726.5	$[PE_2+Na]^+$	■	■	■	■
				748.5	$[PE_2+2Na-H]^+$	■	■	■	■
		PE [16:0 + 18:1]	715.5	738.5	$[PE_3+Na]^+$		■	■	■
				760.5	$[PE_3+2Na-H]^+$	■	■	■	■
0.62±0.03	PG	PG [16:0 + 16:1]	720.5	743.5	$[PG_1+Na]^+$	■	■	■	■
				765.5	$[PG_1+2Na-H]^+$	■	■	■	■
		PG [16:0 + 18:1]	746.5	769.5	$[PG_2+Na]^+$				
				791.6	$[PG_2+2Na-H]^+$	■	■	■	■

EGP: exponential growth phase; SGP: stationary growth phase; GP: glycerophospholipid; PC: phosphatidylcholine; UGP: unknown glycerophospholipid; PE: phosphatidylethanolamine; PG: phosphatidylglycerol.

The glycerophospholipid (GP) composition of MFAF76a, exposed to three concentrations of NO_2 was comparable to that of control sample, exposed to synthetic air (Table 1). PC, PE and PG were found in all experimental conditions. However, one noticeable difference was that an unknown glycerophospholipid (UGP) was not detected in bacteria exposed to 45 ppm of NO_2. This disappearance indicates that this GP is affected by this free radical, as was previously described [17]. An important concentration of NO_2 is necessary to notice the complete disappearance of UGP however, as UGP was still detected after exposure to 0.1 ppm and 5 ppm of NO_2.

The literature reports, that the nitrogen reactive species could mediate the oxidation and/or nitration of membrane GPs, leading to the formation of lipid hydroperoxides, alcohols, and aldehydes [18]. However, no modification of GP m/z was found, indicating that NO_2 does not react with the GPs of MFAF76a in these conditions. However, RNS are described to react with polyunsaturated fatty acids, which are absent from the lipidome of MFAF76a strain. In consequence, the absence of GP reaction with NO_2 appears to be logical. Therefore, the

membrane permeabilization caused by NO_2 (Fig. 2) does not come from alterations of their lipid composition, with maybe the exception of UGP.

To better understand the significance of this lipidic composition shift after bacterial exposure to NO_2, it is necessary to determine the adaptation capabilities of this strain. Therefore, the lipidomic profile of the MFAF76a strain was also followed in two conditions (Table 2) that are known to affect membrane structuration, temperature and growth phase [19], [20]. Bacteria were cultivated at 28°C, the optimal growth temperature of the strain, and 37°C, the temperature of the human body, to observe the modifications that would be necessary for this potential pathogen to infect humans. Lipidomic analysis of the bacteria was then realized either during their exponential growth phase (EGP) or their stationary growth phase (SGP).

Table 2: Effect of temperature and growth phase on glycerophospholipid inventory in *P. fluorescens* MFAF76a strain. The lipid identification was performed on the basis of MS and PSD spectra using LIPID MAPS database and the analysis of lipid standard. The presence of assigned m/z in lipid extract in triplicate is shown by grey squares. The colorless squares show the absence of assigned m/z in lipid extract. The lipid extractions, MS and PSD analysis in all studied conditions were performed in three replicates.

Glycerophospholipid identification						Temperature, °C/growth phase			
						28°C		37°C	
Retention factor	GP class	Species	Molar mass (M), g/mol	m/z	Assignment	EGP	SGP	EGP	SGP
0.24±0.01	PC	PC [16:0 + 16:1]	731.5	732.6	$[PC_1+H]^+$	■	■	■	■
		PC [16:0 + 16:1]	731.5	754.5	$[PC_1+Na]^+$	■	■	■	■
		PC [16:0 + 18:1]	759.6	782.6	$[PC_2+Na]^+$				■
0.26±0.02	UGP	UGP [16:0 + 17:0]	904.5	927.5	$[UGP_1+Na]^+$		■		■
		UGP [16:0 + 18:0]	918.5	941.5	$[UGP_2+Na]^+$		■		■
		UGP [17:1 + 18:0]	930.5	953.5	$[UGP_3+Na]^+$		■		■
0.43±0.02	PE	PE [16:0 + 16:1]	689.5	712.5	$[PE_1+Na]^+$	■	■	■	■
				734.5	$[PE_1+2Na-H]^+$	■	■	■	■
		PE [16:0 + 17:1]	703.5	726.5	$[PE_2+Na]^+$		■		
				748.5	$[PE_2+2Na-H]^+$		■		
		PE [16:0 + 18:1]	715.5	738.5	$[PE_3+Na]^+$	■	■	■	■
				760.5	$[PE_3+2Na-H]^+$	■	■	■	■
0.62±0.03	PG	PG [16:0 + 16:1]	720.5	743.5	$[PG_1+Na]^+$	■	■	■	■
				765.5	$[PG_1+2Na-H]^+$	■	■	■	■
		PG [16:0 + 18:1]	746.5	769.5	$[PG_2+Na]^+$		■		■
				791.6	$[PG_2+2Na-H]^+$	■	■		■

EGP: exponential growth phase; SGP: stationary growth phase; GP: glycerophospholipid; PC: phosphatidylcholine; UGP: unknown glycerophospholipid; PE: phosphatidylethanolamine; PG: phosphatidylglycerol.

Interestingly, the augmentation of temperature did not lead to major differences in GP composition inside the bacterial membrane. However, results show that UGP is not detected in bacteria during the EGP. The lipidic profile of bacteria exposed to NO_2 during the stationary growth phase (Table 1) is therefore very similar to the lipidic profile of bacteria in exponential growth phase (Table 2). During the EGP, bacterial membranes are usually more fluid and disorganized than during the SGP. The shift caused by NO_2 toward an EGP-like lipidic profile could therefore be partially responsible for the constated membrane permeabilization after exposure. This transition could improve bacterial fitness in an environment causing important nitrosative stress.

To respond to environmental stresses, bacteria are not limited to changing the GP makeup of their membranes, but can also modify the degree of saturation of these GP's fatty acids [19], [20]. The global degree of saturation of MFAF76a's fatty acids was determined after exposure to NO_2 or temperature variations at different growth phases (Fig. 3). Bacteria in SGP have an increased degree of saturation compared to bacteria in EGP at both 28°C and 37°C. This modification is coherent with the fact that growth phase can affect the fatty acid saturation of bacterial membranes [21], [22]. Augmentation of the culture temperature from 28°C to 37°C leads to an increase in the degree of fatty acid saturation in the cell membrane.

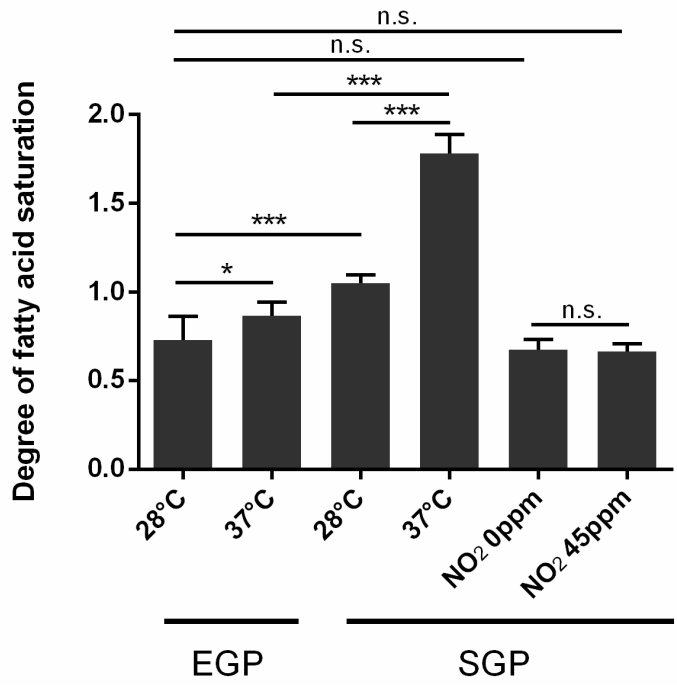

Figure 3: Effects of growth phase, temperature and exposition to NO_2 on fatty acid saturation in MFAF76a strain. Bacterial fatty acids were analyzed and quantified using the GC from at least three independent lipid extracts. NO_2 exposure was done at 28°C. SGP: stationary growth phase, EGP: exponential growth phase. The degree of fatty acid saturation was calculated as the ratio between saturated fatty acids and unsaturated fatty acids, and presented as average value ± SD. Statistical significance was calculated by one way ANOVA. *$P < 0.05$; ***$P < 0.001$; n.s. non-significant.

This augmentation is much more pronounced for the bacteria in SGP than the bacteria in EGP. This result could be expected since saturation of fatty acid allow the cell to compensate for the augmentation of fluidity caused by the augmentation of temperature [20]. NO_2 exposure, however, does not alter the degree of saturation of fatty acids in the MFAF76a strain. Intriguingly, the degree of saturation of bacteria exposed to synthetic air or NO_2 in SGP phase is similar to the degree of bacteria in EGP in liquid culture. Since bacteria were exposed to air only under these two conditions, this particular modification of fatty acid saturation could be the result of this experimental step. Overall, these results suggest that the disappearance of UGP caused by NO_2 may not be the result of a general response of the bacteria to a fluidification of its membrane but rather a specific response to nitrosative stress.

4 CONCLUSION

Here, for the first time, the use of two original exposition systems allowed us to highlight the combined impacts of gaseous NO_2 and UV on bacteria. Firstly, atmospheric NO_2 pollution induces specific effects on bacterial physiology. Exposure to NO_2 or UVB affects bacterial viability. But these two combined stresses do not seem to synergize. This suggests that UV-induced oxidative stress is not important enough to affect bacterial viability or synergize with NO_2 at doses bacteria are susceptible to encounter in the environment. NO_2 alteration of biological membranes seems to be an important component of its effects on bacterial viability, which is not the case for UVB. UVB radiations cause DNA damages, which could lead to bacterial mortality without affecting their membrane permeability. Furthermore, at the membrane level, NO_2 seems to induce responses different from other factors known to alter membrane stability such as temperature and growth phases. Overall, these results demonstrate that air pollution constitutes a unique challenge for bacteria to overcome. Indeed, NO_2 damage biological membranes notably, in ways that other environmental stresses do not.

ACKNOWLEDGEMENTS

This work was conceived by T.C., D.S., S.D., T.K. and C.D.P. We would like to thank N.M.M and H.H. for their help with lipidic studies. We would also like to thank H.H., M.F. and N.O. for critical reading of the manuscript. This study was supported by PhD grants from the GRR SESA (Region Normandie) and was financially supported by the European Union (FEDER), “Région Normandie” and “Evreux Porte de Normandie” (France).

REFERENCES

[1] Skalska, K., Miller, J.S., & Ledakowicz, S., Trends in NOx abatement: A review. *Science of The Total Environment*, **408**(19), pp. 3976–3989, 2010.

[2] WHO, Preventing disease through healthy environments: A global assessment of the burden of disease from environmental risks n.d. http://www.who.int/quantifying_ehimpacts/publications/preventing-disease/en/. Accessed on: 25 May 2020.

[3] Burney, S., Caulfield, J.L., Niles, J.C., Wishnok, J.S. & Tannenbaum, S.R., The chemistry of DNA damage from nitric oxide and peroxynitrite. *Mutation Research*, **424**(1–2), pp. 37–49, 1999.

[4] Möller, M.N., Li, Q., Lancaster, J.R. & Denicola, A., Acceleration of nitric oxide autoxidation and nitrosation by membranes. *IUBMB Life*, **59**(4–5), pp. 243–248, 2007.

[5] Bartesaghi, S. & Radi, R., Fundamentals on the biochemistry of peroxynitrite and protein tyrosine nitration. *Redox Biology*, **14**, pp. 618–625, 2018.

[6] Mullenders, L.H.F., Solar UV damage to cellular DNA: From mechanisms to biological effects. *Photochemical & Photobiological Sciences*, **17**(12), pp. 1842–1852, 2018.
[7] Duclairoir-Poc, C. et al., Airborne fluorescent pseudomonads: What potential for virulence? *International Journal of Current Microbiology and Applied Sciences*, **3**, pp. 708–722, 2014.
[8] Duclairoir-Poc, C. et al., Influence of growth temperature on cyclolipopeptides production and on adhesion behaviour in environmental strains of pseudomonas fluorescens. *Journal of Bacteriology & Parasitology*, **4**(02), 2013.
[9] Kondakova, T. et al., Response to gaseous NO_2 air pollutant of P. fluorescens airborne strain MFAF76a and clinical strain MFN1032. *Frontiers in Microbiology*, **7**, 2016.
[10] Kondakova, T. et al., A new study of the bacterial lipidome: HPTLC-MALDI-TOF imaging enlightening the presence of phosphatidylcholine in airborne Pseudomonas fluorescens MFAF76a. *Research in Microbiology*, 2014.
[11] Bligh, E.G. & Dyer, W.J., A rapid method of total lipid extraction and purification. *Biochemistry and Cell Biology*, **37**(8), pp. 911–917, 1959.
[12] Morrison, W.R. & Smith, L.M., Preparation of fatty acid methyl esters and dimethylacetals from lipids with boron fluoride–methanol. *Journal of Lipid Research*, **5**(4), pp. 600–608, 1964.
[13] Heipieper, H.J., Meulenbeld, G., van Oirschot, Q. & de Bont, J., Effect of environmental factors on the trans/cis ratio of unsaturated fatty acids in Pseudomonas putida S12. *Applied and Environmental Microbiology*, **62**(8), pp. 2773–2777, 1996.
[14] Cadet, J., Douki, T. & Ravanat, J.-L., Oxidatively generated damage to cellular DNA by UVB and UVA radiation. *Photochemistry and Photobiology*, **91**(1), pp. 140–155, 2015.
[15] INERIS, Oxydes d'azote NOx 2011.
[16] Dotterud, L.K., Wilsgaard, T., Vorland, L.H. & Falk, E.S., The effect of UVB radiation on skin microbiota in patients with atopic dermatitis and healthy controls. *International Journal of Circumpolar Health*, **67**(2–3), pp. 254–260, 2008.
[17] Depayras, S. et al., Impact of gaseous NO_2 on p. fluorescens strain in the membrane adaptation and virulence. *International Journal of Environmental Impacts: Management, Mitigation and Recovery*, **1**(2), pp. 183–192, 2018.
[18] Möller, M.N., Lancaster, J.R. & Denicola, A., Chapter 2: The interaction of reactive oxygen and nitrogen species with membranes. *Current Topics in Membranes*, ed. S. Matalon, Vol. 61, Academic Press, pp. 23–42, 2008.
[19] Syakti, A.D. et al., Influence of growth phase on the phospholipidic fatty acid composition of two marine bacterial strains in pure and mixed cultures. *Research in Microbiology*, **157**(5), pp. 479–486, 2006.
[20] Shivaji, S. & Prakash, J.S.S., How do bacteria sense and respond to low temperature? *Archives of Microbiology*, **192**(2), pp. 85–95, 2010.
[21] Larsen, A. et al., The fatty acid profile of vegetative Azotobacter vinelandii ATCC 12837: growth phase-dependence. *Applied Microbiology and Biotechnology*, **68**(4), pp. 548–553, 2005.
[22] Lopes, C. et al., Decoding the fatty acid profile of Bacillus licheniformis I89 and its adaptation to different growth conditions to investigate possible biotechnological applications. *Lipids*, **54**(4), pp. 245–253, 2019.